Exp Brain Res (2006) 171: 283–296
DOI 10.1007/s00221-005-0277-6

RESEARCH ARTICLE

Jing Fan · Jiping He · Stephen I. Helms Tillery

Control of hand orientation and arm movement during reach and grasp

Received: 30 January 2005 / Accepted: 5 September 2005 / Published online: 24 November 2005

Abstract We studied the coordination of arm and wrist motion in a task requiring fine control of hand orientation. Subjects were instructed to reach and grasp one of two targets positioned in the frontal plane at various orientations. The task was performed under three target conditions: fixed orientation, predictably perturbed orientation, and randomly perturbed orientation. For fixed target orientations, the hand began to rotate to the required orientation from the beginning of the reach. Hand peak supination angles scaled linearly with target orientations. The trajectories of hand/arm joint angles also had a one-to-one relationship with different target orientations. These demonstrate that target orientation is a constraint on the hand/arm final orientation, a control variable to be specified in advance by the central nervous system (CNS). Under perturbation conditions, subjects were still able to complete the task smoothly. In the early trials of the predictable perturbation, the hand rotated first to the original target orientation and then corrected for the final target orientation. Initial corrections occurred about 200 ms after the onset of perturbation. This latency decreased as the subjects adapted to the perturbation, and the hand orientation trajectory shifted to match the unperturbed trajectory for the final orientation. By contrast, we observed no clear changes in orientation trajectory under the randomly perturbed conditions. These suggest that feedback control is important to the execution of the movement, but that the CNS tends to optimize feedforward planning rather than feedback correction when the disturbance information is predictable.

J. Fan · J. He (✉) · S. I. H. Tillery
The Harrington Department of Bioengineering, and the Center for Neural Interface Design of the Biodesign Institute, Arizona State University, Tempe, AZ 85287-9709, USA
E-mail: Jiping.he@asu.edu
Tel.: +1-480-9650092

J. He
BioInformatics and BioControl Laboratory, Huazhong University of Science and Technology, Wuhan, China

Keywords Hand orientation · Reach-to-grasp · Perturbation · Neural control · Adaptation

Introduction

Prehension movements involve three components: transport, manipulation, and hand orientation. The transport component moves the hand from an initial position towards the target. The manipulation component controls the finger posture for grasping target objects. The hand orientation component aligns the hand axes, making it convenient to grasp the object. According to the visuo-motor channel hypothesis, prehension movements are controlled by separate channels for reaching and grasping (Jeannerod 1981). The planning of reaching movements is based on the extrinsic properties (direction, distance, etc.) of an object, while grasping is solely concerned with the object's intrinsic properties (shape, size, etc.) (Jeannerod 1981, 1984, 1986). If the channel hypothesis is true, then the transportation of the hand should be independent of the shape or size of the object to be grasped. However, reach and grasp are linked by the movements which define the orientation of the hand. The observation that both transport time and peak velocity can be affected by object size (Marteniuk et al. 1987) provides a hint at how interrelated these independent processes might be, as does the dependence of humeral rotation on object orientation (Marotta et al. 2003).

From the temporal coordination aspect, several principles have been proposed. Jeannerod suggested that a central program imposed temporal constraints to ensure that the time of maximum grasp aperture (MGA) and the onset of the low velocity portion of the transport component were synchronous (Jeannerod 1984). However, only a weak correlation between the timing of MGA and the onset of low-velocity movement was found (Marteniuk et al. 1990). An alternative suggestion is that a strategy based on a simple spatial amplitude ratio determines the relative duration of digit opening and closing in grasping (Mon-Williams and Tresilian 2001). This strategy preserves the idea that prehension is treated by the nervous system as two separable, yet coordinated components. The mechanical component of the coupling between transport and manipulation is the control of hand orientation by wrist and forearm. Hand orientation for grasping is known to depend on the shape (Klatzky et al. 1995) and orientation of the object (Desmurget et al. 1997; Mamassian et al. 1997), leading some to introduce object orientation and hand orientation as a third component of reach-to-grasp (Arbib 1981). However, a study performed by Desmurget et al. (1996) showed that arm transport and hand orientation did not constitute independent visuomotor channels. This suggested interrelationships of hand and arm movements are even stronger in work suggesting that the transport component of a reach-to-grasp is actually directing the motion of the thumb in space (Haggard and Wing 1997; Smeets and Brenner 1999).

To determine the interdependence of these components for the control of reach-to-grasp, we have to first determine how each component is specified. One possibility is that the final posture is determined entirely by the goal of a movement, and that this posture is specified and generated during visually directed movements (Flanders et al. 1992; Helms Tillery et al. 1991). Movement plans are produced online as part of a continuously controlled feedback system (Prablanc et al. 1992; Sabes 2000). This can be modified to accommodate the fact that final postures depend also on starting position (Soechting et al. 1995; Kang et al. 2005) without altering the fundamental principle that the final goal of a movement is the programmed element. The other possibility is that the final posture itself is planned in advance and used as a control variable by the central nervous system (CNS) (Grea et al. 2000).

To investigate how the CNS coordinates hand orientation with arm movement, we designed experiments to study the effects of object orientation during reach-to-grasp movements. We propose that hand orientation is controlled as an individual channel of prehension movements, and that object orientation is an important constraint on that channel.

To force the issue of movement planning, and thereby to more clearly measure independence among these channels, we have applied perturbations to target orientations in the course of reaches. The reaction to target perturbation has traditionally provided a good window into control strategies for motor systems (Georgopoulos et al. 1981; Soechting and Lacquaniti 1983; Goodale et al. 1986; Castiello et al. 1999), and perturbations in general have provided insight into a number of control issues. For example, the reflex responses that maintain an upright stance in the face of sudden and unpredictable translations of a support surface include both spinal and long loop reflexes (Nashner and McCollum 1985). If a subject receives prior information, however, about an upcoming perturbation, an additional anticipatory response develops which provides a more effective control against the perturbation (He et al. 2001). Anticipation can also more directly affect voluntary actions, such as reaching (Weber and He 2004) and ball catching (Button et al. 2002; Lacquaniti and Maioli 1987).

In this paper, we investigated the normal and adapted trajectory of hand orientation in a task requiring a reach-to-grasp of objects with different orientations. We tested movements to targets of fixed orientation, movements to targets with a predictably perturbed orientation, and movements to targets with a randomly perturbed orientation.[1]

Method

Subjects

Five right-handed healthy subjects, three men and two women, aged 23–40, volunteered for this study. All subjects gave written consent to participate in the experiment. The Human Subjects Institutional Review Board of the Arizona State University has approved the experiment protocol and the consent form.

Behavioral apparatus

We designed and built an apparatus (Fig. 1a, b) to investigate the performance of reach-to-grasp task in which target orientation could be quickly changed to perturb the planning or execution of the task. The apparatus consists of a central holding pad that serves as the initial position, and two rectangular targets positioned at approximately shoulder height in the frontal plane. The two targets, one on the left and one on the right, are fitted with touch sensors on both sides of each target. A successful trial is produced by reaching the target and grasping it firmly using a power grip, making contact with both sensors. The movement distance is 32 cm between the center holding pad and the targets. Each target is directly connected to a programmable servomotor that can rotate at up to 900°/s, so a rapid change of the target orientation can be made as a perturbation to the planned prehension task.

Task and experiment

During the experiment, the subject sat in front of the apparatus on an immobilized chair and was instructed to reach and grasp the indicated target using the right hand while maintaining a steady trunk position. Each trial started with a holding phase of 300 ms when the subject placed the fingers on the central holding pad (Fig. 1a). After the holding phase, a target light came on, cueing the subject to reach for the indicated target and make

[1] Some preliminary data have been presented in conferences (Fan et al. 2003).

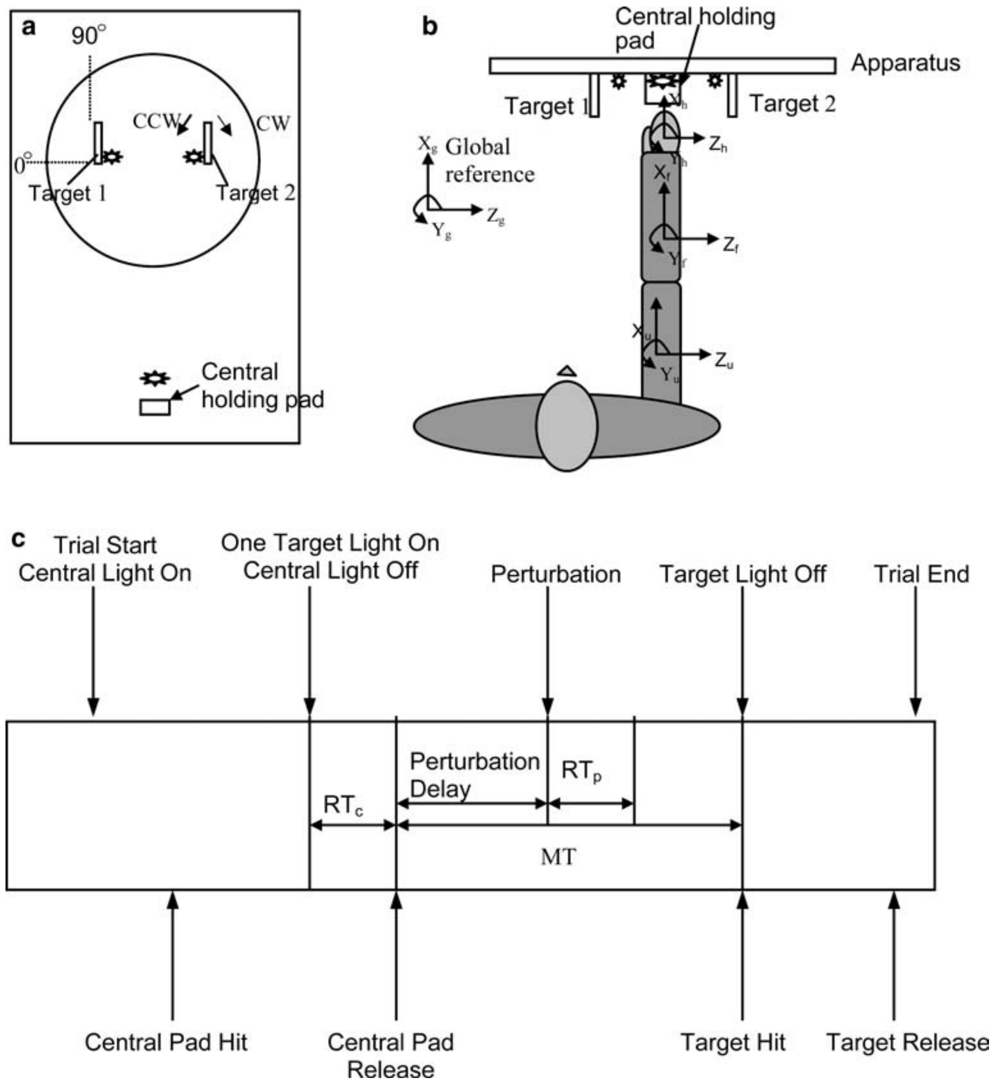

Fig. 1 Experimental setup. **a** The front view of the apparatus: it shows two targets and the target orientation definition. **b** The top view of the experiment setup and the definition of the orthogonal triads. **c** The sequence of events for the reach-to-grasp task and the trial epochs

the grasp. In perturbation trials, the target orientation could change 130 ms after the initiation of the reaching movement. The target light would go off after the grip or the allowed movement time (MT) expired. The subject would return the hand to the central holding pad and wait for the next trial.

The trial epochs are shown in Fig. 1c: cue reaction time (RT_c), MT, perturbation delay, and perturbation reaction time (RT_p). RT_c is the time period from target light ON to reach initiation indicated by release of the central holding pad. The MT is the duration from the central holding pad release to target grasp. Perturbation delay is the time period from the central holding pad release to perturbation onset. The RT_p is the duration from the perturbation onset to the instant when there was a detectable deviation in the trajectory of hand orientation to accommodate the new target orientation (defined later in Fig. 7).

Each subject performed ten sets of trials. Table 1 shows the target orientations for each set during the experiment. The first seven sets consisted of movements towards seven fixed target orientations: 30°, 50°, 70°, 90°, 110°, 130° and 150° (Fig. 1a shows the angle definition). The order of the orientations in the first seven sets was randomly selected for each subject. The last three sets were perturbation trials where the target orientation was either repeatedly (eighth and ninth sets) or randomly (tenth set) rotated from its initial orientation at vertical (90°). In the eighth set, target 1 was rotated 30° clockwise (CW) 130 ms after holding pad release, while target 2 was rotated at 30° counterclockwise (CCW). In the ninth set, target 1 was perturbed at 30° CCW, while target 2 was perturbed at 30° CW.

In the tenth set, there were three different cases for each target. The targets were randomly perturbed either 30° CW, 30° CCW, or non-perturbed (i.e., the target would stay at 90°). Perturbation delay was always 130 ms. We set the six movements to the two targets as one block, with each target having three movements (one for each case). The order of the targets and cases within each block were randomly selected. So each case has 33.3% chance to occur for each target.

Table 1 Target orientation used in the experiment

	Target 1	Target 2
Normal trials		
Set 1	90°	90°
Set 2	50°	130°
Set 3	110°	70°
Set 4	150°	30°
Set 5	70°	110°
Set 6	130°	50°
Set 7	30°	150°
Repeat perturbation trials		
Set 8	90° with 30° CW perturbation	90° with 30° CCW perturbation
Set 9	90° with 30° CCW perturbation	90° with 30° CW perturbation
Random perturbation trials		
Set 10	90°, 30° CW, 30° CCW	90°, 30° CW, 30° CCW

Each subject was required to perform five movements to each target under each condition as described above. Subjects 4 and 5 voluntarily performed two more repetitions for a total of 7. All data from every subject were analyzed and summarized.

Baseline and 3D movement recording

During the experiment, arm and hand movement were recorded by an optical motion capture system (OPTOTRAK, Northern Digital Inc.). Each of the three arm segments, including hand, forearm and upper arm, was marked with three infrared emitting diodes (sampling rate at 100 Hz). Given the 3D position of the markers at any given instant, we computed three sets of three mutually orthogonal unit vectors. These unit vectors comprised the segment marker axes expressed in the global reference frame.

The global reference frame is defined by a right-handed orthogonal triad of unit vectors fixed on the apparatus, where y_g denotes the vertical axis; x_g defines the horizontal direction from subject to the apparatus, and z_g is defined by the cross product of x_g and y_g (Fig. 1b).

A set of right-handed orthogonal triads affixed to each arm segment defines the bone axes of that segment (Fig. 1b). To use the 3D positions of the markers to track the anatomical axes for each segment, the rotation matrix from the bone axes to the marker axes must be determined. This requires simultaneous knowledge of marker positions and bone axes, which is accomplished by recording a baseline. During baseline posture, the subject held the arm horizontally in a parasagittal plane, and with his palm toward the ground. Thus the segment anatomical axes align with the global reference coordinate. The baseline rotation matrix from marker coordinates to the global coordinates equals the rotation matrix from segment marker coordinates to segment bone coordinates (Carhart 2000).

In this paper, we analyzed five joint angles of the distal arm. Hand pronation–supination is defined as hand rotation about the forearm (X_f axis). Hand adduction–abduction is defined as hand rotation about the Y_f axis. Forearm rotation about the X_u axis is humeral rotation. Forearm rotation about the Y_u axis is forearm flexion–extension. In addition, we define hand rotation about the X_g axis as "global hand rotation" (see Fig. 1b for the axes).

Results

Kinematic characteristics of non-perturbed trials

Overall, stereotypical hand pronation–supination trajectories during reaching to grasp targets with fixed orientation are observed in all subjects. Typical examples of these trajectories are shown in Fig. 2. Plot (a) and (b) each shows five consecutive movements of subject 1 to the left and the right target fixed at 50°. Plot (c) and (d) each shows five consecutive movements of subject 3 to the left and the right targets fixed at 110°. The traces are aligned on the central holding pad release (stars), and the circles indicate the moment of target hit. There is an obvious target dependent variation in hand pronation–supination trajectories in subject 1: the hand tends to pronate after the central holding pad release during movements to the left target (a), but not to the right target (b). However, this characteristic is only observed in subject 1 for target orientations $<70°$ but not for orientation angles $\geq 70°$. For all other subjects, the trajectory difference is less observable and can be illustrated by the trajectory from subject 3 to targets oriented at 110° as shown (c and d). To further study the trajectory differences caused by target locations, we plotted average trajectories from all five subjects for the left (e) and the right (f) targets oriented at 50 and 110°, respectively. Comparing these two plots, we found that when the two targets were fixed at 110°, the average trajectories were quite similar. For 50°, however, instead of a quick supination in the early phase of the movement as shown by the average trajectory to the right target (f), the hand supinated slowly to reach the left target (e).

For each of the two targets and different fixed orientations, movement durations were very consistent with less than 5% variation for each subject. For fixed orientation $\geq 70°$, the trajectories were also consistent

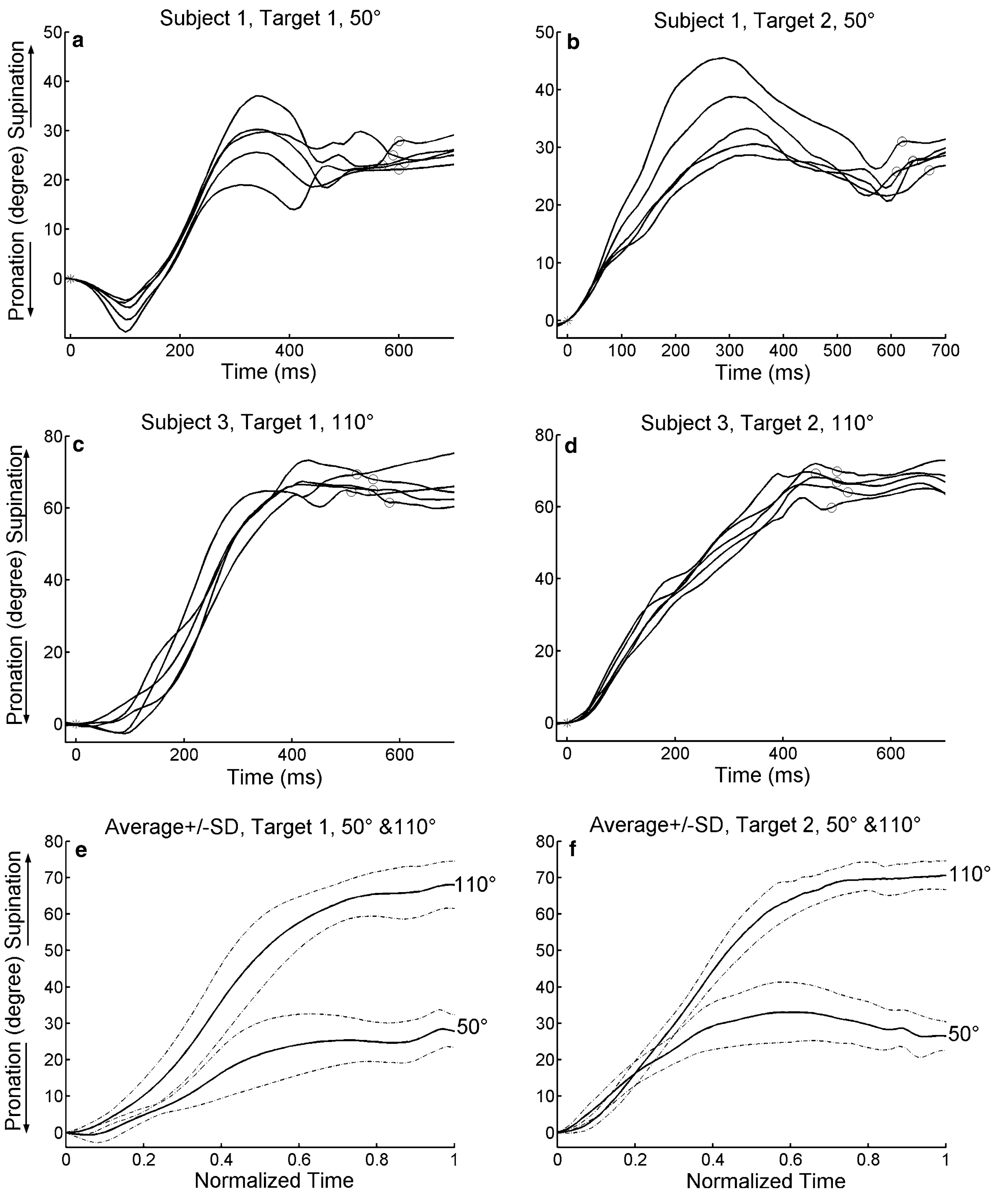

Fig. 2 General nature of hand pronation–supination during non-perturbed trials. Five consecutive movements of subject 1 to the left (**a**) and right (**b**) targets oriented at 50°; five consecutive movements of subject 3 to the left (**c**) and right (**d**) targets oriented at 110°. The traces are aligned on the central pad release (*stars*), and the *circles* indicate target hit. Average trajectories (with standard deviation) of the five subjects for the 50 and 110° targets are shown in plot (**e**) (target 1) and (**f**) (target 2). Due to different movement durations of the five subjects, we normalized their MT in each trial before averaging the curves. Time zero is center pad release. Time one represents target hit time

among all subjects as shown in Fig. 2. During movement to fixed target orientations, we sometimes observed overshooting in hand supination (Fig. 2a, b). In the example shown, the subject first supinated the hand until overshooting the required orientation for grasp, and then pronated back to match the target orientation before grasp. Based on this observation, it seemed possible that peak supination would show only minimal dependence on target orientation. To test this, we calculated the mean for the peak supination time and peak supination amplitude of the five subjects according to target orientation (Fig. 3). Both peak supination time and peak supination had linear relationships with target orientation.

Figures 4a–e show the average hand and arm orientation trajectories during the first seven non-perturbed sets for the right target. Each curve is averaged from the trajectories of all repetitions to the same target orientation by subject 1. Figure 4f shows the distance from the hand to the target. The trajectory is averaged from five non-perturbed trials to the same target oriented at 90°. Most transport motion is completed at 400 ms after movement initiation. Grasp (contact with both surfaces of the rods) occurs around 600 ms after movement onset. Hand pronation–supination, hand adduction–abduction, global hand rotation, and humeral rotation, and forearm flexion–extension all varied significantly with target orientation measured 250 ms after movement initiation (Table 2). This indicates that both wrist and elbow are used by the CNS to adjust hand orientation according to target orientation. Both hand and arm joint angles have a one-to-one relationship with different target orientations.

Averaged wrist transport velocity profiles to different fixed orientations of the right target for the same subject are shown in Fig. 4g. Each line is averaged from five trials of movements to the same orientation. Time zero is central pad release. The wrist velocity profiles show no clear dependence on target orientation. The statistical analysis shows that target orientation has no significant effect on wrist tangential velocity (Table 2), indicating that the transport motion is not affected by target orientation.

We further calculated the mean time taken to reach peak angular acceleration of hand pronation–supination and humeral rotation of the five subjects (Fig. 5). For each of the seven target orientations, the time to peak acceleration always occurred earlier for humeral rotation than for hand pronation–supination. The time of peak acceleration for humeral rotation was 25–40 ms after movement initiation, while that for hand pronation–supination was 45–65 ms. Thus elbow rotation always led wrist rotation in our task. Figure 5a also shows that target orientation does not have a significant effect on the time to reach peak acceleration. The individual time variations of each joint angle are small. However, the peak angular acceleration amplitude of hand pronation–supination and humeral rotation both have an approximately linear relationship with target orientation (Fig. 5b). Larger target orientation calls for greater angular acceleration. All the peak accelerations occur during the first quarter of the reach duration, which suggests that the visual information for the object orientation was taken into account at the very beginning of the prehension movement.

Perturbation responses

Hand pronation–supination for movements to target 2 perturbed at 30° CCW for subject 2 is shown in Fig. 6. In both repeated (Fig. 6a) and random (Fig. 6b) perturbation trials, perturbations occurred 130 ms after central pad release, as shown by stars.

After the central pad release, the subject began a movement towards the original 90° target orientation. About 200 ms delay after perturbation onset, the subject began a corrective movement to bring the hand into alignment with the new target orientation. The final hand orientation from the perturbation trials was about

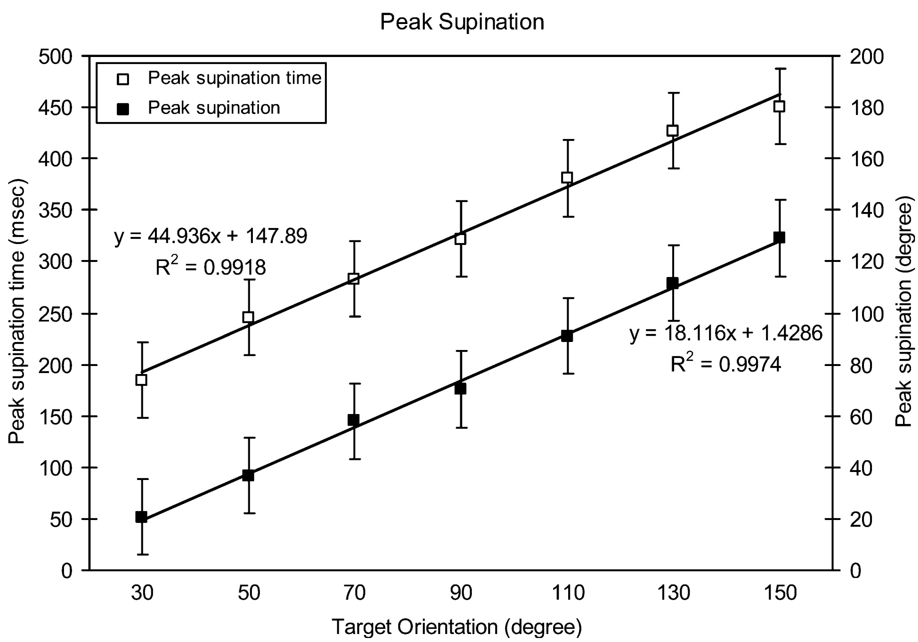

Fig. 3 Peak supination. Mean (± SE) for the peak supination time (the left *Y* axis) and amplitude (the right *Y* axis) of the five subjects, according to target orientation

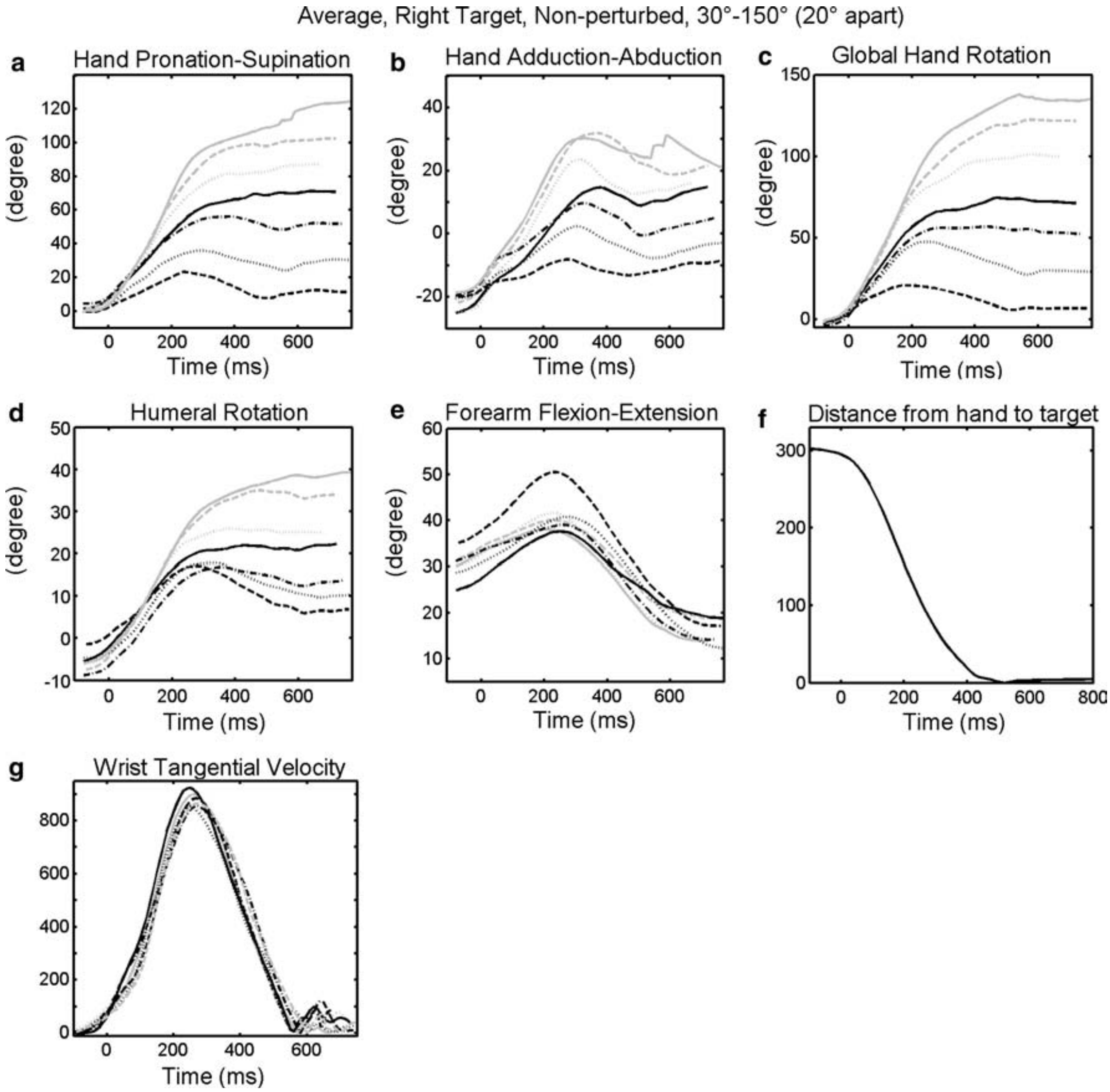

Fig. 4 Dependence of movement parameters on target orientation. **a**–**e** Averaged hand and arm rotation trajectories during the first seven non-perturbed sets of subject 1. The types of those curves represent target different orientations: *black dashed* (30°), *black dotted* (50°), *black dash-dot* (70°), *black solid* (90°), *gray dotted* (110°), *gray dashed* (130°), *gray solid* (150°). **f** Distance from the hand to the target during unperturbed movements. **g** Averaged wrist transport velocity profiles to different fixed orientations of the same target for a representative subject. Each line is averaged from five trials of movements to the same target fixed at the same orientation. The representation of the line types is the same as plot **a**–**e**

Table 2 Results of statistical analyses of the variables involved in movements during non-perturbed trials of subject 1

Variables	$F_{(7,28)}$	P
Hand pronation–supination	386.49	$<<0.01$
Hand adduction–abduction	82.06	$<<0.01$
Global hand rotation	508.85	$<<0.01$
Humeral rotation	63.07	$<<0.01$
Forearm flexion–extension	14.13	<0.01
Wrist tangential velocity	0.77	$=0.6022$

The seven different orientations were considered as seven levels ($a=7$). The five movements to the same oriented target were considered as five repetitions ($n=5$). All variables were measured 250 ms after movement initiation

the same as the final hand orientation reached during unperturbed trials to the same final target orientation. In the repeat perturbation trials (Fig. 6a), the rotation decreased and the correction started earlier over trials, as the hand orientation trajectory shifted gradually towards that required for the final target orientation. No clear orientation trajectory adaptation was observed in the random-perturbed trials (Fig. 6b). The movement duration of the repeat-perturbed trials was not significantly different from those of the non-perturbed trials ($F_{(1,19)}=0$, $P=0.9654$ for the CW repeat-perturbed trials; $F_{(1,19)}=0.02$, $P=0.8841$ for the CCW repeat-perturbed trials).

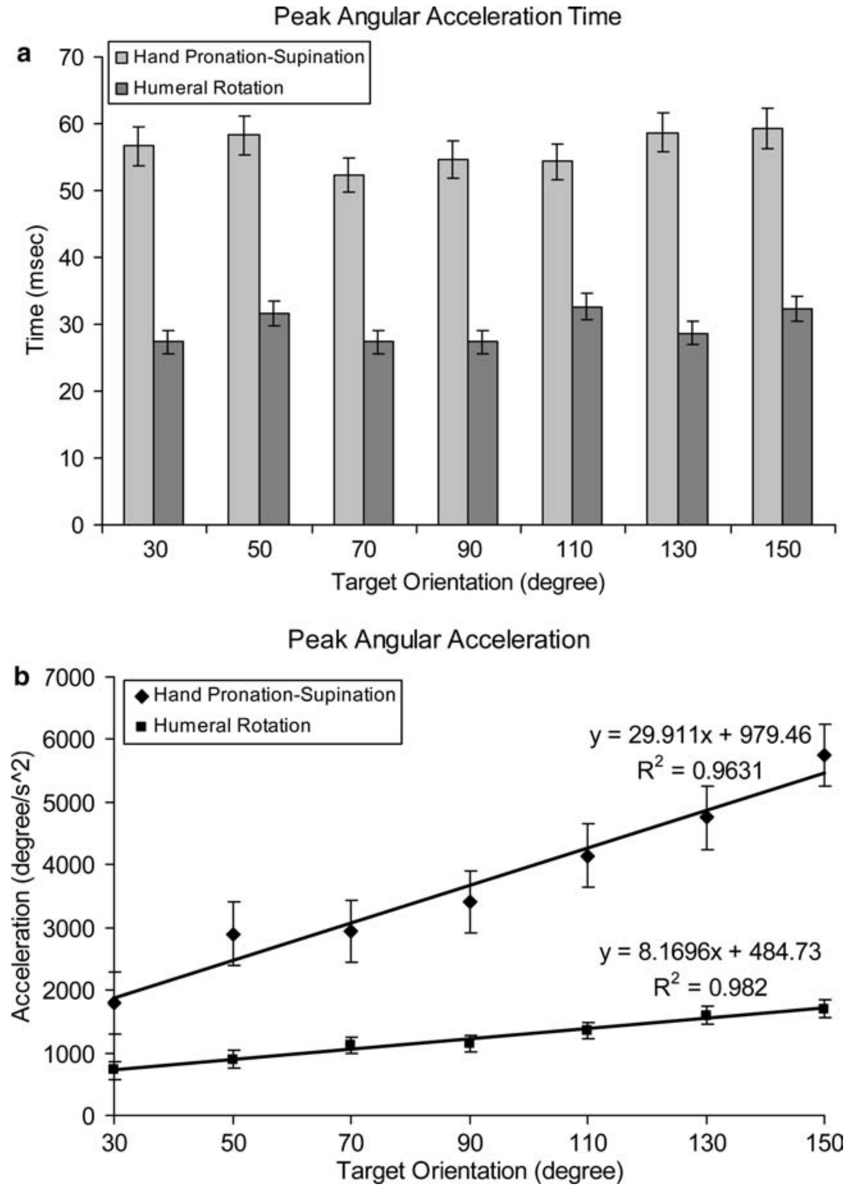

Fig. 5 Peak angular acceleration. **a** Mean (±SE) for the peak angular acceleration time of the five subjects, according to target orientation. **b** Mean (±SE) for the peak angular acceleration of the five subjects, according to target orientation

To further investigate the perturbation effects, we calculated the RT_p during the perturbation trials for each subject. We defined the RT_p as the time from the perturbation onset to the instant when the trajectory of any movement parameter started to deviate from the average trajectories recorded when reaching for fixed 90° non-perturbed orientation. Here, we used global hand orientation because this parameter had the greatest range. To compute RT_p, we first normalized all of the 90° trials to have duration and final amplitude of 1, and computed mean trajectories (see Fig. 7a, c). All trajectories from the perturbation trials were then normalized with respect to the average trajectory to 90° orientation from non-perturbed trials: both MT and the amplitude were normalized to have a final end point scaled with respect to the average from 90° orientation (Fig. 7a, c). The stars represent perturbation onsets. The zone between the upper dashed curve and the lower dashed curve is the 95% confidence interval (CI) to the 90°-oriented target motion. Once the trajectory is moving out of this zone and without reentry, it is 95% certain that the subject is not moving to the 90° target. However, the trajectories start to shift from the 90° trajectories well prior to leaving the CI. To find that point, we calculated the peak acceleration in appropriate direction along the trajectory before it left the zone (Fig. 7b, d). For CCW perturbation, negative peak acceleration was used to determine the deviation point as the hand pronated. For CW perturbation, positive peak acceleration was used to determine the deviation point as the hand supinated. We defined the normalized RT_p as the time taken from perturbation onset to the acceleration peak which drives the hand to align with the target. The normalized RT_p multiplied by the movement duration of the 90° average trials is the real RT_p.

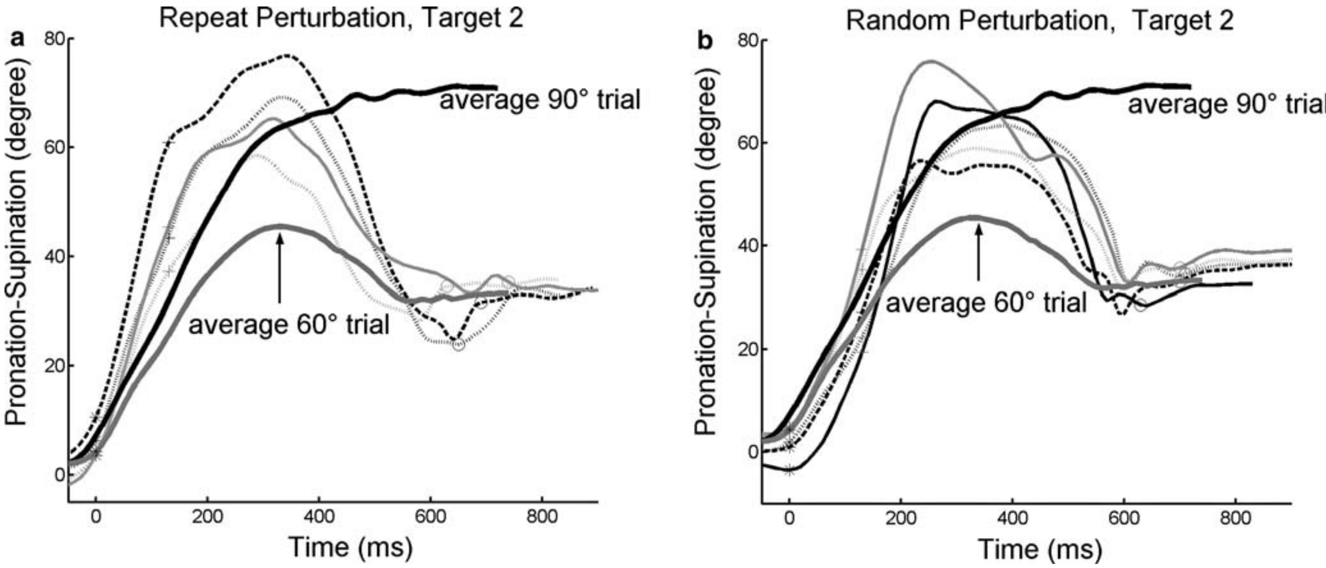

Fig. 6 General nature of perturbation responses. Hand pronation–supination trajectories for movements to the right target perturbed at 30° CCW (from 90 to 60°) of subject 2. **a** Four repeatedly perturbed movements (due to losing markers in the first trial); **b** Five randomly perturbed movements. The line representation is: *black solid* (first trial), *black dashed* (second trial), *black dotted* (third trial), *gray solid* (fourth trial), *gray dotted* (fifth trial). The *black thick dashed curves* are averaged from those non-perturbed trajectories with target oriented at 90°, while the *gray thick dashed curves* are averaged 60° (mean of the average 50 and 70° trajectories) (corresponding with target final orientation of 30° CCW). The *star marks* indicate the central pad release. The *plus signs* indicate the perturbation onset. The *circles* indicate target hit

The mean RT_p of the five subjects for each repeatedly perturbed condition across consecutive trials is shown in Fig. 8. Each marker shows the mean RT_p of the five subjects of that trial for one repeat perturbation condition. Different marker types represent different repeat perturbation conditions. The horizontal lines show the mean RT_p (the middle line) of the five subjects for the randomly perturbed (non-predictable)

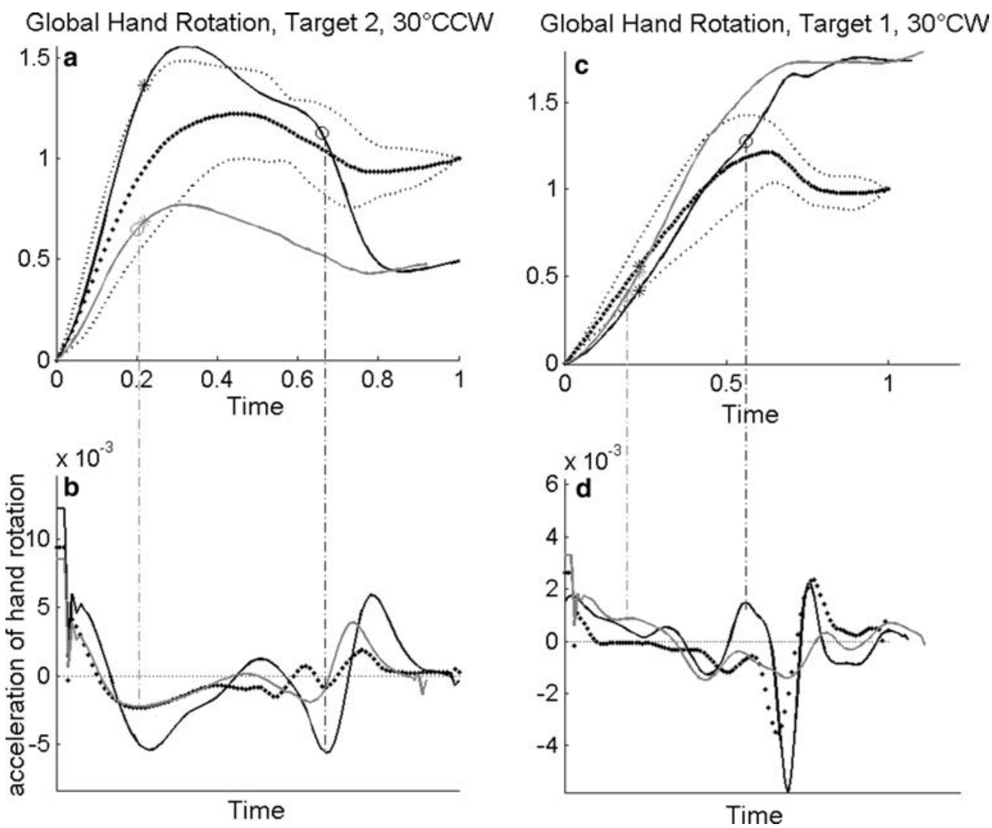

Fig. 7 RT_p calculation illustration. This figure shows normalized global hand rotation (**a**, **c**) and acceleration (**b**, **d**) during repeat-perturbed trials of subject 5. The *thick dotted curves* are averaged from 90° non-perturbed trajectories. The *two dashed curves* show 95% CI of the 90° non-perturbed trajectories. The color index is: *black* is the first trial, and *gray* is the seventh trial. The *stars* indicate onset of perturbation. The *circles* indicate the deviation points determined by the acceleration peaks

Fig. 8 Mean RT_p of the five subjects for different perturbation conditions across consecutive trials. The horizontal lines show the mean RT_p (*middle*) for the randomly perturbed (non-predictable) trials of the five subjects with 95% CI (*top* and *bottom lines*). Each marker shows the mean RT_p of the five subjects of that trial for one repeat perturbation condition with standard error. The mean RT_p of trial 6 and trial 7 were averaged from subject 4 and subject 5. Different kinds of markers represent different repeat perturbation conditions

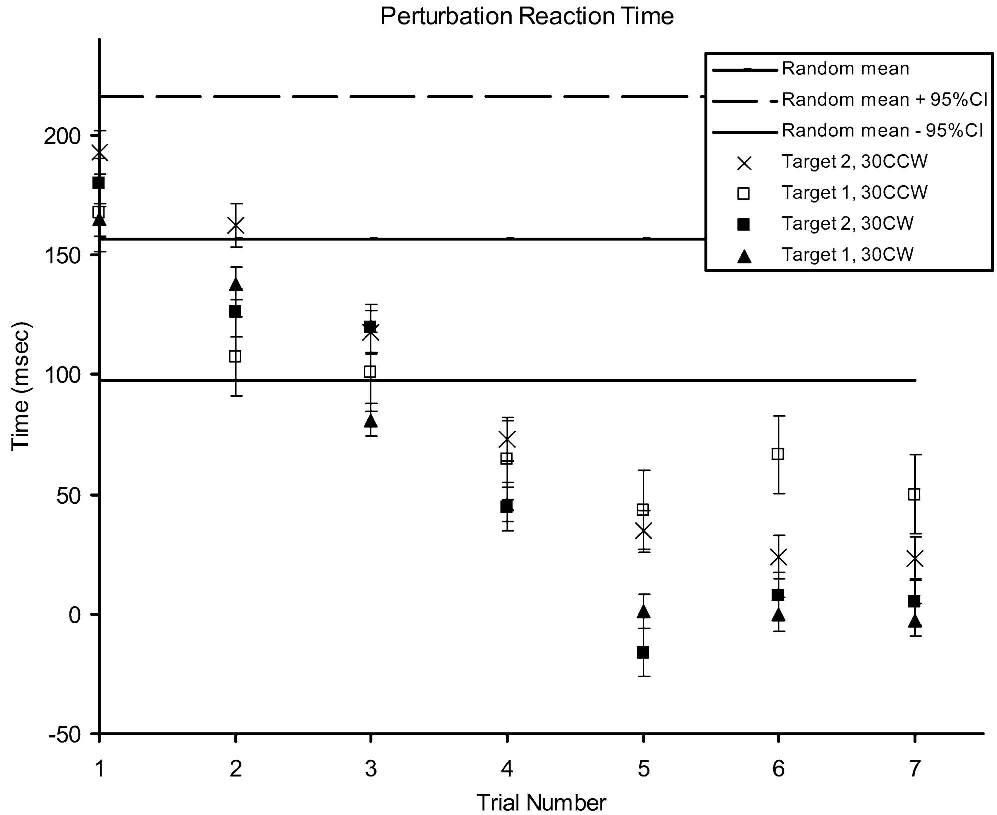

trials with 95% CI (upper and lower lines). An RT_p less than the 95% CI bound (the lower line) is indication of the subject predicting the perturbation. As shown in this figure, for all the four repeat-perturbation conditions, the five subjects were able to predict the perturbation after only two or three trials, indicated by sharp decreases in RT_p. For some orientations, the RT_p was close to even less than zero, meaning that the subject's trajectory was detectably different from the mean trajectory to the vertical target prior to the perturbation.

That the subjects were able to anticipate the orientation of the target following the predictable perturbation suggests that they were planning a movement to a target whose orientation was not actually present. This could imply either a mental rotation, or simply a recollection that the final target orientation for the upcoming movement was not as presented. If the subjects are performing a mental rotation, one might expect to see changes in the RT_c as they begin to take the rotation into account prior to initiating movement. The RT_c across trials for six different conditions is shown in Fig. 9. The RT_c for the perturbation trials is clearly affected by which perturbation condition applies ($F_{(5,36)} = 5.05$, $P = 0.0013$), with larger reaction times for both repeat perturbation conditions than for either the random perturbation or non-perturbed conditions. Despite the apparent increase in RT_c across trials for the repeat perturbation conditions, there was not a significant effect of trial number ($F_{(6,35)} = 0.52$, $P = 0.7913$).

Discussion

The present study was conducted to examine the interdependence of hand and arm orientations and their control mechanisms during reach-to-grasp. We found that for fixed target orientations, the final orientations reached by the hand and arm depended strongly on target orientations. The final orientations to be reached determined the trajectories of each joint angle. However, the transport velocity did not change with the change of target orientations. These results indicate that transport and orientation are different effectors, which favor the three-component hypothesis (Arbib 1981) that prehension movements consist of three channels: transport, manipulation, and orientation. Our perturbation studies showed that during random perturbations, the motor system was able to update the target orientation during the course of motion. During repeat perturbations, subjects were able to anticipate the perturbation and plan a movement to a target that was not actually present, their RT_p dropped dramatically and the RT_c increased, suggesting a longer time to activate a more complex plan.

Relationship between hand orientation, arm movement and target orientation

Previous studies found that hand azimuth for grasping depends primarily on movement direction (Bennis et al.

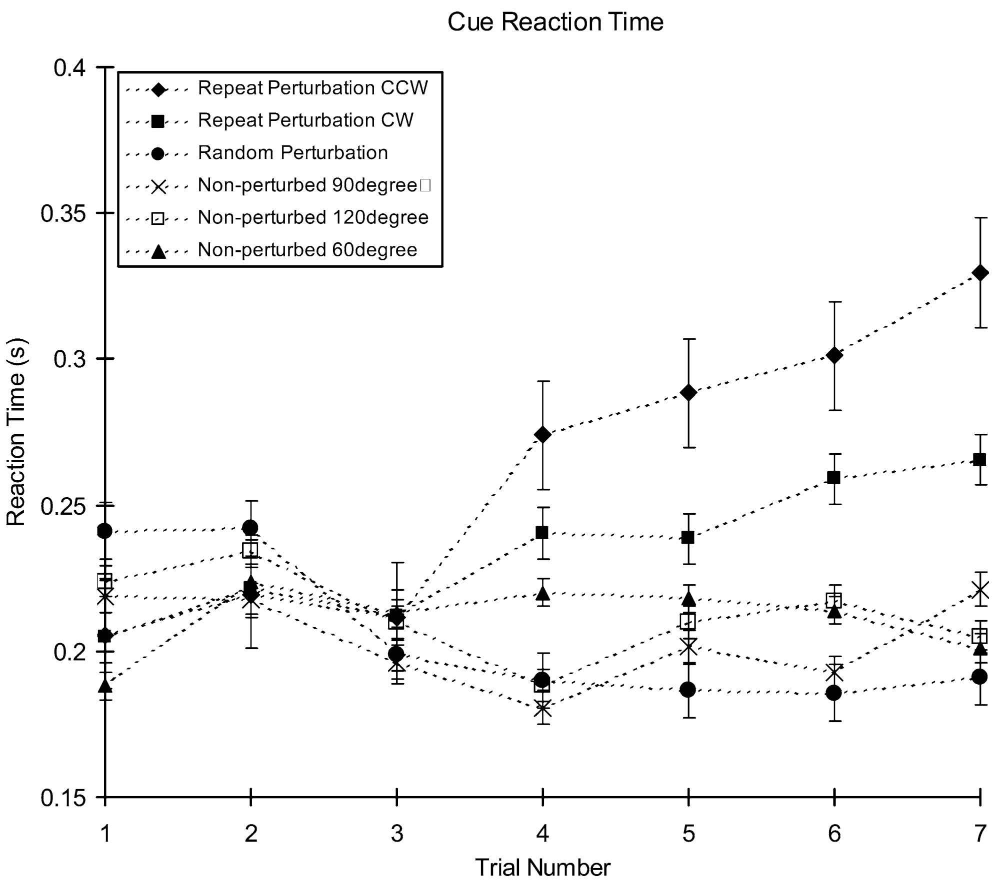

Fig. 9 Mean RT_c of the five subjects for different conditions across consecutive trials. Each curve shows the mean RT_c (±SE) of the five subjects across consecutive trials for one condition. RT_c of the non-perturbed 120° trials (corresponding to the final target orientation of the CW perturbation) were averaged from the RT_c of the non-perturbed 110° trials and 130° trials. Likewise, RT_c of the non-perturbed 60° (corresponding to the final target orientation of the CCW perturbation) trials were averaged from the RT_c of the non-perturbed 50° trials and 70° trials. The mean RT_c of trial 6 and trial 7 were averaged from subject 4 and subject 5

2002). However, hand azimuth only shows the projection of hand orientation on the horizontal plane. In our experiments, we studied the effect of object orientation on hand and arm joint angles during 3-D prehension movements. We fixed initial hand position and target locations to keep the movement direction fixed, and investigated the 3-D movements to targets oriented at various angles. We found that hand pronation–supination and humeral rotation varied significantly with the target orientation. In our tasks, the orientation of the hand was set primarily by three anatomical rotations: hand pronation–supination, hand adduction–abduction and humeral rotation. Hand flexion–extension did not co-vary with target orientation. Only the trajectories to the 30°-oriented target were significantly different for forearm flexion–extension. The trajectories of forearm flexion–extension to other six orientations did not have a significant difference ($F_{(6,24)} = 1.74$, $P = 0.1647$). This may be because forearm flexion–extension to 30°-oriented target is at the extreme of the comfortable range. The final hand orientation is parallel with target orientation, which shows that object orientation is directly coupled with hand orientation at the time of grasping. Although some have concluded that the posture for grasping is due to geometrical constraints expressed by coupling between hand orientation and movement direction (Bennis et al. 2002), our data suggests that object orientation is also an important constraint during the 3-D prehension movements as suggested in previous work (Grea et al. 2000; Elsinger and Rosenbaum 2003).

In our task, the subjects were free to move their limbs in any way they chose to grasp the objects, and generally five of the seven available degrees of freedom (dof) of the upper limb were used to grasp the targeted object. Due to the redundancy, the desired final hand position and orientation can be obtained through an infinite number of arm joint configurations. However, our data shows that hand and arm orientation trajectories are reproducible from trial to trial for the same target orientation and starting position. The movement duration in different trials for each case is also very consistent. The trajectories of hand pronation–supination, hand adduction–abduction and humeral rotation have a one-to-one relationship with different target orientations. The results are compatible with the posture control hypothesis which states that the final posture reached by the upper limb should be invariant when the context in which the movement is performed is stable (Flanders et al. 1992). Prehension movements are planned as a transition between the arm initial angular configuration and a target posture defined by a transformation of object characteristics into a set of arm and hand angles.

The time to peak acceleration of both hand pronation–supination and humeral rotation occurred during the first quarter of the reaching motion. The amplitude of peak acceleration of both joint angles has an approximately linear relationship with target orientation. Larger orientations required greater peak acceleration. These indicate that the visual information for the object orientation was taken into account at the very beginning of the prehension movement. This conclusion is compatible with previous findings that the representation of a visual target in extra personal space has to be transformed into a kinesthetic representation of arm segment orientation before a goal-directed movement can be implemented (Helms Tillery et al. 1991). This suggests that the final posture to be reached is a control variable specified in advance by the CNS. The same conclusion was reached by other studies (Grea et al. 2000; Elsinger and Rosenbaum 2003). Elsinger and Rosenbaum suggested that subjects relied on feedforward modeling of prospective movements as they selected end postures prior to overt movement production. They also mentioned that the orientation control depended in some aspect on the final posture to reach after the grasping movement (Elsinger and Rosenbaum 2003).

In these non-perturbed trials, hand and arm orientations changed significantly with the changes of target orientation. However, no change was observed in the transport velocity during movements to all the seven different target orientations. This is in contradiction to the suggestion that the position and orientation of the hand in space are unlikely to be controlled through separate independent neural pathways (Desmurget et al. 1998). Our results favor the three-component hypothesis (Arbib 1981) rather than the two-channel hypothesis (Jeannerod 1981). Prehension movements consist of three channels: transport, manipulation, and orientation. Within the orientation component, postural control is used so that the one-to-one relationship exists between target orientation and hand/arm posture. The final posture to be reached is a control variable specified in advance by the CNS, which determines the angular trajectories. The isochrony principle (Fitts 1954) of point-to-point movements can also be extended to the orientation component: average angular velocity increases with increase in object orientation so that movement duration is only weakly affected by object orientation. In our tasks, the elbow always rotated before wrist rotation. The individual time variations of each joint angle are small. Latash also observed this proximal-to-distal order of elbow and wrist joint involvement in his study of simple reaction time (Latash 2000).

Here, we cannot rule out any spatial control hypothesis since we did not manipulate object location. We suggest that spatial control may be the control mechanism implemented within the transport channel. This has a computational validation, as demonstrated by the Hoff–Arbib model for prehension (Hoff and Arbib 1993). This model had two independent channels for transport and aperture, which were compatible with the visuomotor channel hypothesis. While that model accounted for the kinematic characteristics of the arm trajectory corrections, it did not consider orientation. Here, we suggest that transport, orientation, and manipulation should be considered as three different components. Spatial control is used by the transport component to deal with the hand/arm trajectory in relation to object location, whereas postural control is implemented by the orientation component to adjust hand/arm orientation with object orientation. Our results provide support for a recent theory of goal-oriented behavior that implements an example of such motions with a model of orientation-matching (Torres and Zipser 2002, 2004). In this model, the intended location and orientation are simultaneously transformed into a matching postural goal, thus allowing online update of the location and orientation in the presence of perturbations that occur after movement initiation.

Perturbation responses

The kinematics of hand orientation are sensitive to perturbation of the target during the prehension movements. Over-rotation (relative to final orientation) was observed in both repeat perturbation trials and random perturbation trials. After perturbation, when the intial target orientation was changed, subjects were able to smoothly correct the movements during execution, showing that reaching and grasping movements can be corrected online. Moreover, the final hand orientation for the perturbation trials was the same as that reached when the object was initially oriented along the final orientation during the unperturbed trials. This again confirmed the postural control hypothesis.

In the repeat perturbation trials, both MT and the over-rotation decreased over trials as the control system learned the perturbation and adapted to its effect. Hand orientation trajectory shifted to match the unperturbed trajectory for the final orientation. In all the four repeat perturbation conditions, all the five subjects showed prediction after two or three trials: the subjects knew that the target orientation was going to change, and they knew where the final target orientation would be. So their RT_p decreased dramatically, and sometimes even became negative. But RT_c was clearly longer for the repeatedly perturbed condition. In the random perturbation trials, the system was able to respond at a suitable latency to the changed task contingencies. But no clear orientation trajectory adaptation was observed. The RT_p in the random perturbation trials did not decrease over trials as the subjects could not predict the perturbation. Therefore, subjects were forced to react to the perturbations during the movement (online correction).

The online (feedback) trajectory control requires that visually guided reaching begins with the selection of a target from the visual scene and the formation of a movement plan. In such models, the feedback controllers are not only responsible for the initial target selection and formulation of an execution plan, but also play an ongoing role throughout the movement (Sabes 2000). In some cases, the feedback system behaves as if it were two separate systems: a fast feedback control loop driven by the visual feedback information, and a slow mechanism which is under cognitive control (Pisella et al. 2000). The predictable perturbation presents the neural control system with the opportunity to adapt the control strategy and update the internal model for the perturbation, while the unpredictable perturbation prevents such adaptation from occurring and forces the neural control system to utilize feedback control. The current results suggest that feedback control is important for the complete and smooth execution of the movement, but that the system really is designed to optimize feedforward planning rather than feedback correction when the disturbance information is predictable. The CNS shifts its control emphasis from visual feedback to predominantly a feedforward strategy when the demands of the motor task are known in advance. The feedforward model plays the dominant role in producing accurate control of movement. When the difficulty of the task increases, the CNS might recruit an online feedback control mechanism. Here lies the possibility that both types of mechanisms coexist in the CNS, yet the recruitment of one versus the other in a controlled setting will be a function of the task difficulty, of the priorities of multiple competing performance goals, and familiarity or knowledge of the task and environment.

Acknowledgements The work is supported in part by a grant from DARPA (MDA972-00-1-0027) and by funding from the Biodesign Institute at the Arizona State University.

References

Arbib MA (1981) Perceptual structures and distributed motor control. In: Brooks VB (ed) Handbook of physiology, Section 1, vol 2, Part 2. William & Wilkins, Baltimore, pp 1449–1480

Bennis N, Roby-Brami A (2002) Coupling between reaching movement direction and hand orientation for grasping. Brain Res 952:257–267

Button C, Davids K, Bennett SJ, Savelsbergh GJP (2002) Anticipatory responses to perturbation of co-ordination in one-handed catching. Acta Psychol 109:75–93

Carhart MR (2000) Biomechanical analysis of compensatory stepping: implications for paraplegics standing via FNS. PhD dissertation. Arizona State University, pp 80–95

Castiello U, Bennett K, Bonfiglioli C, Lim S, Peppard RF (1999) The reach-to-grasp movement in Parkinson's disease: response to a simultaneous perturbation of object position and object size. Exp Brain Res 125(4):453–462

Desmurget M, Prablanc C (1997) Postural control of three dimensional prehension movements. J Neurophysiol 77:452–464

Desmurget M, Prablanc C, Arzi M, Rossetti Y, Paulignan Y, Urquizar C (1996) Integrated control of hand transport and orientation during prehension movements. Exp Brain Res 110(2):265–278

Desmurget M, Grea H, Prablanc C (1998) Final postural of the upper limb depends on the initial position of the hand during prehension movements. Exp Brain Res 119:511–516

Elsinger CL, Rosenbaum DA (2003) End posture selection in manual positioning: evidence for feedforward modeling based on a movement choice method. Exp Brain Res 152(4):499–509

Fan J, Helms Tillery SI, He J (2003) Hand orientation and perturbation effects during reaching and grasp. In: Presentation at the 25th annual international conference of the IEEE EMBS, Cancun, Mexico

Fitts PM (1954) The information capacity of the human motor system in controlling the amplitude of movement. J Exp Psychol 47:381–391

Flanders M, Helms Tillery SI, Soechting JF (1992) Early stages in a sensorimotor transformation. Behav Brain Sci 5:309–362

Georgopoulos AP, Kalaska JF, Massey JT (1981) Spatial trajectories and reaction times of aimed movements: effects of practice, uncertainty, and change in target location. J Neurophysiol 46:725–742

Goodale MA, Pelisson D, Prablanc C (1986) Large adjustments in visually guided reaching do not depend on vision of the hand or perception of target displacement. Nature 320(6064):748–750

Grea H, Desmurget M, Prablanc C (2000) Postural invariance in three-dimensional reaching and grasping movements. Exp Brain Res 134:155–162

Haggard P, Wing A (1997) On the hand transport component of prehensile movements. J Mot Behav 29:282–287

He JP, Maltenfort MG, Wang QJ, Hamm TM (2001) Learning from biological control systems: modeling neural control of posture and movement. Control Syst Mag 21(4):55–69

Helms Tillery SI, Flanders M, Soechting JF (1991) A coordinate system for the synthesis of visual and kinesthetic information. J Neurosci 11:770–778

Hoff B, Arbib M (1993) Models of trajectory formation and temporal interaction of reach and grasp. J Mot Behav 25(3):175–192

Jeannerod M (1981) Intersegmental coordination during reaching at natural visual objects. In: Long J, Baddeley A (eds) Attention and performance. Erlbaum, Hillsdale, pp 153–168

Jeannerod M (1984) The timing of natural prehension movements. J Mot Behav 16:235–254

Jeannerod M (1986) The formation of finger grip during prehension. A cortically mediated visuomotor pattern. Behav Brain Res 19(2):99–116

Kang T, Helms Tillery SI, He J (2005) Determining natural arm configuration along a reaching trajectory. Exp Brain Res (in press)

Klatzky RL, Fikes TG, Pellegrino JW (1995) Planning for hand shape and arm transport when reaching for objects. Acta Psychol (Amst) 88(3):209–232

Lacquaniti F, Maioli C (1987) Anticipatory and reflex coactivation of antagonist muscles in catching. Brain Res 406:373–378

Latash ML (2000) Modulation of simple reaction time on the background of an oscillatory action: implications for synergy organization. Exp Brain Res 131(1):85–100

Mamassian P (1997) Prehension of objects oriented in three-dimensional space. Exp Brain Res 114:235–245

Marotta JJ, Medendorp WP, Crawford JD (2003) Kinematic rules for upper and lower arm contributions to grasp orientation. J Neurophysiol 90:3816–3827

Marteniuk RG, MacKenzie CL, Jeannerod M, Athenes S, Dugas C (1987) Constraints on human arm movement trajectories. Can J Psychol 41:365–378

Marteniuk RG, Leavit JL, MacKenzie CL, Athenes S (1990) Functional relationships between grasp and transport components in a prehension task. Hum Mov Sci 9:149–176

Mon-Williams M, Tresilian JR (2001) A simple rule of thumb for elegant prehension. Curr Biol 11:1058–1061

Nashner LM, McCollum G (1985) The organization of human postural movements: a formal basis and experimental synthesis. Behav Brain Sci 8:135–172

Pisella L, Grea H, Tilikete C, Vighetto A, Desmurget M, Rode G, Boisson D, Rossetti Y (2000) An 'automatic pilot' for the hand in human posterior parietal cortex: toward reinterpreting optic ataxia. Nat Neurosci 3:729–736

Pranblanc C, Martin O (1992) Automatic control during hand reaching at undetected two-dimensional target displacements. J Neurophysiol 67:455–469

Sabes PN (2000) The planning and control of reaching movements. Curr Opin Neurobiol 10:740–746

Smeets JB, Brenner E (1999) A new view on grasping. Motor Control 3:237–271

Soechting JF, Lacquaniti F (1983) Modification of trajectory of a pointing movement in response to a change in target location. J Neurophysiol 49:548–564

Soechting JF, Buneo CA, Herrmann U, Flanders M (1995) Moving effortlessly in three dimensions: does Donders' law apply to arm movements? J Neurosci 15:6271–6280

Torres EB, Zipser D (2002) Reaching to grasp with a multi-jointed arm. I. Computational model. J Neurophysiol 88:2355–2367

Torres EB, Zipser D (2004) Simultaneous control of hand displacements and rotations in orientation-matching experiments. J Appl Physiol 96:1978–1987

Weber DJ, He JP (2004) Adaptive behavior of cortical neurons during a perturbed arm-reaching movement in a nonhuman primate. Prog Brain Res 143:477–490